Accepted Manuscript

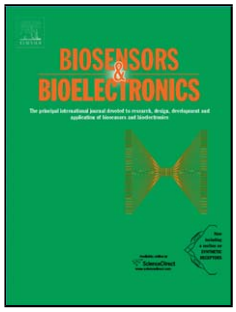

Title: Impedance biosensing using phages for bacteria detection: Generation of dual signals as the clue for in-chip assay confirmation

Authors: M.B. Mejri, H. Baccar, E. Baldrich, F.J. Del Campo, S. Helali, T. Ktari, A. Simonian, M. Aouni, A. Abdelghani

PII: S0956-5663(10)00355-6
DOI: doi:10.1016/j.bios.2010.06.054
Reference: BIOS 3861

To appear in: *Biosensors and Bioelectronics*

Received date: 12-4-2010
Revised date: 9-6-2010
Accepted date: 25-6-2010

Please cite this article as: Mejri, M.B., Baccar, H., Baldrich, E., Del Campo, F.J., Helali, S., Ktari, T., Simonian, A., Aouni, M., Abdelghani, A., Impedance biosensing using phages for bacteria detection: Generation of dual signals as the clue for in-chip assay confirmation, *Biosensors and Bioelectronics* (2010), doi:10.1016/j.bios.2010.06.054

Impedance biosensing using phages for bacteria detection: Generation of dual signals as the clue for in-chip assay confirmation

M B Mejri[1,4], H Baccar[1], E Baldrich[2*], F J Del Campo[2], S Helali[1], T Ktari[1], A Simonian[3], M Aouni[4], A Abdelghani*[1]

[1] National Institute of Applied Science and Technology, Nanotechnology Laboratory, Centre Urbain Nord, Bp676, 1080 Charguia cedex, Tunisia

[2] Institut de Microelectrònica de Barcelona (IMB-CNM), CSIC, Campus Universitat Autònoma de Barcelona, Barcelona 08193, Spain

[3]Materials Engineering, Auburn University, Auburn AL, 36849, USA

[4] Faculté de Pharmacie, 5000 Monastir, Tunisie

*** Corresponding authors**:

* A. Abdelghani. National Institute of Applied Science and Technology, Bp676, Centre Urbain Nord, 1080 Charguia Cedex, Tunisia. Tel.: +216 71703829; fax: +216 71 704329. E-mail address: aabdelghan@yahoo.fr

* E. Baldrich. Institut de Microelectrònica de Barcelona (IMB-CNM), CSIC, Campus Universitat Autònoma de Barcelona, Barcelona 08193, Spain. Tel.: +34 93 5947700x1306; fax: +34 93 58014 96. E-mail address: eva.baldrich@imb-cnm.csic.es

Abstract:

In the present work, we compare the use of antibodies (Ab) and phages as bioreceptors for bacteria biosensing by Electrochemical Impedance Spectroscopy (EIS). With this aim, both biocomponents have been immobilised in parallel onto interdigitated gold microelectrodes. The produced surfaces have been characterised by EIS and Fourier Transform Infra-Red (FTIR) Spectroscopy and have been applied to bacteria detection. Compared to immunocapture, detection using phages generates successive dual signals of opposite trend over time, which consist of an initial increase in impedance caused by bacteria capture followed by impedance decrease attributed to phage-induced lysis. Such dual signals can be easily distinguished from those caused by non-specific adsorption and/or crossbinding, which

helps to circumvent one of the main drawbacks of reagentless biosensors based in a single target-binding event. The described strategy has generated specific detection of *E. coli* in the range of 10^4 - 10^7 CFU mL^{-1} and minimal interference by non-target *Lactobacillus*. We propose that the utilization of phages as capture biocomponent for bacteria capture and EIS detection allows in-chip signal confirmation.

Keywords: Interdigitated Gold Microelectrodes, T4-Phage, *E. coli*, *bacteria* reagentless biosensing, Impedance Spectroscopy

1. Introduction

In spite of the medical advances occurred over the last decades, bacterial pathogens are still among the main cause of death in the world. The ability of microorganisms to evolve extraordinarily fast may partly account for this, but changes in the population cultural habits, as well as technological and medical advances, have deeply influenced pathogen prevalence and distribution. The increasing mobility of the population worldwide, the unrestrained use of antibiotics, the use of modified microorganisms *in field*, or the possibility to suffer bioterrorist attacks are just examples of new concerns. Ironically, water and food, which are essential resources for life, account among the main vectors of infection transmission. Each year, food and waterborne pathogens are responsible for massive public health costs, including sick days, medical expenses, and preventable deaths. About 1.1 billion people have no access to drinking water in developing countries and waterborne diseases are estimated to kill around 1.8 million worldwide (U.S. Centers for Disease Control and Prevention. Atlanta 2006). These epidemics are not limited to developing countries. A water-transmitted *Cryptosporidium* outbreak occurred in Milwaukee (USA) in 1993 resulted in more than 400,000 infected persons (Mac Kenzie et al., 1994), and foodborne pathogens are believed to cause 76 million infections, 323,000 hospitalizations and 5,000 casualties per year in the USA (Tauxe 2002), and were responsible for at least 387,000 zoonotic infections in the European Union only in 2005 (Norrung and Buncic 2008). Timely pathogen detection is thus an essential priority for public protection and any newly developed technology able to perform fast, simple and efficient determination of pathogen presence will be directly applicable to a variety of fields, including clinical microbiology, food industry and environmental monitoring.

Electrochemical Impedance spectroscopy (EIS) is a powerful electrochemical technique capable of detecting small changes occurring at the solution-electrode interface. Accordingly, EIS has been extensively exploited for the characterisation of materials and surface modification procedures, and well as for the monitoring of binding events. The fact that impedance measurements can be performed in a reagentless assay format makes it very attractive for biosensor development (Daniels and Pourmand 2007; Panke et al., 2008). The equipment required is compact, does not contain mobile parts, and is easy to miniaturise, suggesting that EIS biosensors could be easily used *in-field* with minimal requirements.

Furthermore, impedance combines rapid response, low detection limits, cost-effectiveness, and the possibility of performing *real-time* monitoring of the samples, in contrast to established strategies for pathogen detection such as culture, polymerase chain reaction (PCR), enzyme linked immunosorbent assay (ELISA), or those sensors based on sandwich assay formats.

A number of authors have exploited EIS for pathogen detection, either by monitoring the changes in the medium conductivity caused by bacterial growth/metabolism, or the changes in the solution-electrode interface due to microorganism non-specific adsorption or specific capture onto the sensor surface (Muñoz-Berbel et al., 2008; Varshney and Li 2009). Reagentless EIS immunosensing of bacterial whole cells using interdigitated microelectrodes has generated detection limits down to 10^4 CFU mL^{-1} for *E. coli* and *Salmonella typhimurium* assayed in saline solution (Radke and Alocilja 2005; Laczka et al., 2008). In these works, bacteria captured on top of or between the electrode fingers behaved as insulator elements and negatively affected electron transfer. Detection in more complex matrices, such as culture media or in the presence of non-target bacteria, generated a large background signal, attributed by the authors to biocomponent non-specific adsorption onto the sensor surface. Detection in real sample matrices has worked better on macroelectrodes, which performance is less negatively affected by surface blocking procedures and non-specific adsorption (Pournaras et al., 2008; Das et al., 2009)

The main limitation of reagentless sensors based on a single capture/biorecognition event, on the other hand, is that non-specific adsorption of non-target sample components onto the sensor surface can generate false positive results, negatively affect the limit of detection, and/or interfere with signal transduction (Radke and Alocilja 2005; Radke and Alocilja 2005; Laczka et al., 2008). Attempts to improve detectability and selectivity through target pre-concentration or signal enhancement have been made by using antibody (Ab) -functionalised magnetic particles and nanoparticles, as well as enzyme-labelled Ab (Ruan et al., 2002; Kim et al., 2007; Varshney et al., 2007), although not always providing appropriate negative controls. Nevertheless, even if sandwich-based sensors produce high selectivity and detectability, they entail many incubation and washing steps, long assays, and are extremely difficult to automate.

Shabani and co-workers proposed a unique alternative for EIS bacteria biosensing, based on the use of bacteriophages, instead of Ab, crosslinked to the surface of carbon screen printed

electrodes (Shabani et al., 2008). Bacteriophages are viruses that attach and infect bacteria with high specificity. The infection cycle starts with phage binding to specific receptors on the bacterial surface, subsequent injection of the phage genome, followed by production of high numbers of phage components (nucleic acids and structural/enzymatic proteins) by the host cell, and release of new phages and phage components into the medium. Accordingly, phage production is possible in an easier, faster, and cheaper way than Ab production and does not depend on the use of animals, which makes them promising tools in biosensing (Balasubramanian et al., 2007; Lakshmanan et al., 2007). In their work, Shabani et al performed EIS measurements on phage-captured bacteria, after allowing infection to proceed for 25 minutes. Interestingly, they registered not only an increase in electrolyte resistance caused by the bacterial insulating effect, but also a simultaneous decrease in charge-transfer resistance for increasing bacteria concentrations. This result opposes the effect generated by just cell capture and was attributed to the release of ions caused by phage-induced bacteria lysis and concomitant increase in medium conductivity at the electrode vicinity. The sensor had a reported detection limit of 10^4 CFU mL^{-1} in saline buffer, in an assay of about 40 minutes.

We now go a step further. In this work we demonstrate that EIS monitoring over time using bacteriophages for bacteria detection generates successive dual signals of opposite trend, enabling in-chip detection confirmation. In this respect, specific capture generates an initial increase in impedance, which is followed by an impedance decrease due to phage-induced lysis. These signals can be easily distinguished from those caused by non-specific adsorption and/or crossbinding. Coupled to the use of interdigitated microelectrode arrays, this strategy allowed *E. coli* detection with a limit of detection of 10^4 CFU mL^{-1}, and with minimal interference from non-target *Lactobacillus*.

2. Materials and Methods

2.1. Interdigitated Gold Microelectrode Microfabrication

Interdigitated microelectrodes were produced by standard photolithographic techniques and extensively characterised as described in (Laczka et al., 2008). Briefly, a micron thick silicon

oxide layer was thermally grown over a four-inch silicon wafer. Next, the electrodes were patterned by a lift-off technique. This consisted in the deposition of a photoresist over the wafer, which was then exposed through a suitable quartz-chromium mask. After developing the resist, the wafer was metallised by sputtering. This metal layer was composed by 10 nm titanium, 10 nm nickel and 100 nm gold. Nickel acts as diffusion barrier to avoid the formation of undesirable Ti-Au alloys. After the metallisation, the wafer was immersed in an acetone bath where the excess resist was removed, leaving the microelectrode structures neatly defined on the wafer. The next step consisted in depositing a passivation layer to protect the contact lines of the devices. This was a mixed layer of silicon oxide (4000 Å) and silicon nitride (7000 Å). After this, the wafer was newly coated in photoresist and insulated through a second mask that defines the final electrode geometry and contact pads. After the resist was developed, it was hardened by soft bake in order to withstand the etching steps that followed. The passivation layer was etched in a reactive ion etching step, followed by a wet etching step that removed any traces of silicon oxide from the surface of the electrodes.

Last, the wafers were diced into 3 × 3 mm individual chips, which were then transferred and wire bonded to suitable print circuit boards (PCB). The encapsulating resin used to protect the connection pads of the PCB and wire bonds was an Epotek thermocurable polymer (Epotek H-77). Each chip features two interdigitated gold electrodes, each of them consisting of 54 fingers 10μm wide, separated 10μm from the nearest band.

Before their utilisation, the electrodes were electrochemically activated by applying series of potential pulses (10 s each) at 0 and −2V (vs. an external Ag/AgCl reference electrode) in 0.5M $NaNO_3$ solution. The degree of activation was then verified by cyclic voltammetry in 1mM potassium ferrocyanide ($K_4Fe(CN)_6$). A chip was considered active and suitable for impedance measurements when the cyclic voltammograms of its two electrodes were similar and presented two peaks (oxidation and reduction) in the ferrocyanide solution.

2.2. Bacteria culture

E. coli K12 cells, provided by BioPhage Pharma (Montreal, Canada), were grown at 37ºC in Luria-Bertani (LB) liquid medium for 8-10 h. *Lactobacillus plantarum* cells were grown at 37ºC in MRS broth for 18-20 h. In addition to nutrients and a pH buffer, MRS broth also contains sodium acetate to prevent growth of competing bacteria. The cultures were

spectrophotometrically monitored (OD 600 nm) in order to estimate bacterial total count, followed by serial dilution and plating on LB/MRS-agar plates to obtain the viable counts (colony forming units [CFU]). For the preparation of bacterial suspensions of different concentrations, bacterial cultures were centrifuged at 6200 rpm for 5 min. The pellets were then washed twice, followed by re-suspension and serial dilution in sterile PBS (140mM NaCl, 2.7mM KCl, 0.1mM Na_2HPO_4 and 1.8mM KH_2PO_4, pH 7.2).

2.3. T4-Phage culture

T4 phage, which specifically infects *E. coli*, was obtained from BioPhage Pharma (Montreal, Canada). *E. coli* K12 liquid culture, grown until the exponential phase was reached, was inoculated with 500 µl of a phage T4 stock solution. The suspension was incubated at 37 °C in a rotary shaker (200 rpm) for three hours. Chloroform was added to final 10% (v/v) and the solution was kept at 4°C for 20 min. It followed ultrafiltration through a sterile 0.2 µm filter and centrifugation at 4°C (19000 g). The purified phages were resuspended in sterile PBS, serially diluted, and titrated by the double layer procedure (serial decimal phage dilutions were prepared from initial phage suspension, 100µl from each one and 400µl of *E.coli* suspension in exceptional phase (DO=0.3) were added to semi-liquid medium LB (agar 7.5g/l). The mixture was suddenly added on solid medium and incubated in 37°C for 24 hours. The titration is then executed by direct counting of lysis plaques). The phage stock produced in this way was at an approximate titter of 10^7 plaque forming units per millilitre (PFU mL^{-1}).

2.4. Bioreceptors Physisorption on Interdigitated Gold Microelectrodes

Unless otherwise stated, incubations were carried out inside a homemade humid chamber, which consisted in a closed container enclosing a damp paper towel, in order to prevent evaporation and preserve biocomponent's integrity.

For surface modification with phages, 100 µL of the T4-phage stock solution (10^7 PFU mL^{-1}) were deposited onto the interdigitated gold microelectrodes, followed by incubation at 37ºC for 90 min.

The antibodies (Ab) used were anti-*E. coli* goat polyclonal IgG (ab13627) purchased from Abcam (UK, United Kingdom). For surface immuno-functionalisation, Ab were diluted in PBS to a final concentration of 5 µg mL^{-1} and 100 µL were deposited onto each interdigitated gold microelectrode, followed by incubation at 37ºC for 90 min.

In both cases, after modification with the appropriate biocomponent, the chip was submitted to extensive washing with sterile PBS. A volume of 100 µL of BSA solution (1% (w/v)) was then deposited on top of the modified substrate and was incubated for 30 min at 37ºC. This blocking step was intended to prevent successive non-specific adsorption of non-target biocomponents (Figure 1).

2.5. Electrochemical Impedance Spectroscopy

The electrochemical measurements were performed at room temperature in a conventional one-compartment voltammetric cell with a three electrode configuration. We used an Autolab302N impedance analyser (Ecochemie, The Netherlands) equipped with the NOVA1.4 acquisition software. The impedance spectra were obtained in a frequency range from 100 mHz to 100 kHz, using a modulation voltage of 5 mV. One of the two interdigitated gold microelectrodes in a chip (0.00405 cm^2) was used as the working electrode, platinum foil (1 cm^2, Ecochemie, Netherland) was used as a counter electrode, and an Ag/AgCl (Ecochemie, The Netherlands) was used as reference electrode. Unless otherwise stated, electrochemical measurements were carried out in sterile PBS and inside a Faraday cage. The PBS sterile solution contained 140 mM NaCl, 2.7 mM KCl, 0.1 mM Na_2HPO_4, and 1.8 mM KH_2PO_4 and had a conductivity of 14.73 mS cm^{-1}. Mineral water, obtained from a local provider (Melina, Tunisia, 355 mg L^{-1} bicarbonate; 120.2 mg L^{-1} calcium; 9.80 mg L^{-1} sulfate; 8.4 mg L^{-1} magnesium; 53.30 mg L^{-1} chlorures; 23 mg L^{-1} sodium; 0.3 mg L^{-1} fluorures; 16 mg L^{-1} nitrates; 1.60 mg L^{-1} potassium) with a conductivity of 0.56 mS cm^{-1} was alternatively used as water sample matrix.

2.6. Fourier Transform Infra-Red spectroscopy (FTIR)

T4 phage physisorption onto gold surface has been additionally confirmed by Fourier-Transform Infra-Red (FTIR) spectroscopy which was performed with a Brucker IFS 66/S spectrometer equipped with a MIR (Middle Infra-Red) source, a DTGS detector, and a KBr separating mirror. All spectra are collected with 64 scans for the reference and the sample, with 4 cm^{-1} resolution in a vacuum of 0.003 bars. First, we recorded the spectrum of the naked gold electrode (after cleaning) as reference, and then that of gold electrode with immobilized T4 phage as a sample. The ratio between reference and sample spectra gives information about the T4 phage layer immobilised on the gold surface.

3 Results and Discussion

3.1. Electrochemical Characterisation of Interdigitated Gold Microelectrodes

The microelectrodes used in this work were produced by standard photolithographic techniques. Each chip featured two interdigitated gold microelectrodes, each of them consisting of 54 fingers 10 µm wide, separated 10 µm from the nearest band. Work started with chip characterisation in order to test signal reproducibility between microelectrodes.

Typical cyclic voltammograms recorded for the two interdigitated gold microelectrodes of a chip in $NaNO_3$ solution containing potassium ferrocyanine ($K_4Fe(CN)_6$) can be found in the supplementary material. A reversible redox wave is observed, with oxidation and reduction peaks around 0.3 and 0.2 V (vs. Ag/AgCl) respectively. The two voltammograms are nearly indistinguishable, which indicates that the two microelectrodes of the chip exhibit equivalent active surfaces and good gold quality.

The impedance spectra independently recorded for the two microelectrodes (of the same chip) at 0 V in PBS solution are also presented in the supplementary material. The impedance spectra of the two microelectrodes are nearly identical, which evidences the high quality and reproducibility of the gold surface. More details concerning the structure, characterisation and

electrochemical performance of these microlectrodes can be found in the work published by Laczka et al., 2008 (Laczka et al., 2008).

3.2. Production and characterisation of functionalised microelectrodes

3.2.1. Physisorption of T4-Phage onto gold microelectrodes

Random physisorption is the easiest and fastest strategy for biomolecule immobilisation onto physical substrates. Chiefly, physisorption does not require biocomponent biotinylation, chemical modification, or the utilisation of cross-linkers, and does not depend on multi-step and long experimental procedures. Even if a variable fraction of the immobilised biocomponents loses its function (Butler 2000; Heitz and Van Mau 2002), physisorbed Ab have been described to perform better for whole bacteria detection than Ab immobilised via more complex strategies, such as cross-binding onto self-assembled monolayers (Baldrich et al., 2008; Laczka et al., 2008). This is beside the fact that physisorption almost certainly prevents an orderly orientation of the phages. In addition, physisorbed phages have been described to promote bacteria specific capture, infection and lysis, when monitored by surface plasmon resonance (SPR) (Balasubramanian et al., 2007).

Physisorption was thus selected in this work for transducer functionalisation based on its simplicity. For their modification with phages, microelectrodes were incubated at 37ºC for 90 min in the presence of T4-phage (100 μL, 10^7 PFU mL^{-1}), followed by washing and physical blocking with BSA. Blocking prevented non-specific adsorption of unwanted non-target components during subsequent incubations. Figure 2 shows the impedance spectra recorded in sterile PBS solution for interdigitated gold microelectrodes either bare or modified with T4-phage/BSA. Typical Nyquist diagrams of the different interfaces were obtained. The immobilisation of T4-phage and BSA layers induce an increase in the diameter of the semicircle component of the Nyquist plot, indicative of augmentation of the electron-transfer resistance. This behaviour is consistent with the successful immobilisation of T4-phage and BSA molecules, which hinder migration of the redox probe towards the electrode surface.

The stability of the T4-phage layer blocked with BSA was verified over time. Figure 2 inset shows the variation of the impedance for a microelectrode modified with T4-phage and BSA,

registered over 2 hours in sterile PBS buffer at 233 mHz. An initial increase in impedance was observed for the first 30 minutes, presumably due to the rearrangement of the proteins on the gold surface. It followed signal stabilisation, which remained constant for 5 hours (data not shown).

3.2.2. FTIR characterisation of phage-modified microelectrodes

Gold electrodes (5mm x 5 mm), modified with phages (but not BSA), were additionally studied by FTIR spectroscopy. The FTIR spectrum of the T4-phage layer immobilised on the gold surface, obtained between 500 and 4000 cm^{-1}, is given as supplementary material. The immobilisation of T4-phage is confirmed by the presence of a number of peaks, which are indicative of the presence of organic matter. For instance, the peaks between 500 and 950 cm^{-1} are assigned to stretch mode of C-S and C-C groups. The peak between 1250 and 1500 cm^{-1} correspond to methyl symmetric and antisymmetric bending mode. The peaks between 1700 and 1750 correspond to the vibrational stretching mode of C=O. The appearance of a broad absorption band between 2750 and 2000 cm^{-1} is attributed to (NH_2) hydrogen bond symmetric and asymmetric vibrations (Bhaskaran et al., 2007). Moreover we observe small peaks at 2800-2950 cm^{-1} which are assigned to the vibration mode of alkyl chains (Kohli et al., 1998). These results confirm the immobilisation of T4-phage onto the gold surface.

3.2.3. Negative control microelectrodes modified with Ab

It was necessary to confirm that the signal trends observed for bacteria detection on T4-phage-modified microelectrodes were truly induced by successive cell attachment, infection, and lysis and not just an artefact (for example caused by bacteria natural death and/or desorption). Ab was expected to induce bacteria binding, but not their later disruption.

For this reason, microelectrodes were modified in parallel by physisorption of anti-*E. coli* Ab in place of phages. As before, chips were next washed and blocked with BSA in order to prevent non-specific adsorption. Impedance measurements were performed before and after antibody immobilisation on interdigitated gold microelectrodes. Figure 3 presents the Nyquist plots obtained for interdigitated gold microelectrodes with and without Ab and BSA. The increase in the Nyquist spectra is interpreted by the successful immobilisation of Ab and saturation of non-specific sites with BSA. Interestingly, it can be observed that at low

frequencies, the impedance variation due to Ab/BSA immobilisation is bigger than the change registered for T4-phage (with BSA), which indicates that higher surface coverage and/or biomolecule packing is attained with antibody. This is presumably related to the relative size of the two components, as a T4 unit is on average 10 times bigger than an Ab molecule (200 nm long and 80-100 nm wide for T4, compared to approximately 15x15x3 nm for Ab).

3.3. Bacteria EIS biosensing at microelectrodes modified with phages or Ab

We next studied the response over time of gold microelectrodes, modified with Ab or phages and blocked with BSA as previously described, in the presence of *E. coli*. Negative controls were performed in parallel by incubating *E. coli* with microelectrodes modified with just BSA (but neither Ab nor phages), as well as by incubating phage- or Ab-modified microelectrodes in the presence of non-target bacteria (*Lactobacillus*).

The typical response of EIS immunosensors in the presence of target *E. coli* is illustrated in Figure 3. The curve shows the absolute variation of the impedance (ΔZ) versus the incubation time at fixed frequency (233 mHz). ΔZ is calculated as $|Z - Z_0|$, where Z is the value of the impedance module of the immunofunctionalised microelectrode after bacteria binding and Z_0 is the value of the impedance module of that immunofunctionalised microelectrode previous to bacteria capture. The occurrence of specific immunodetection is characterised by two consecutive signal trends. We first observe a linear increase in impedance due to the specific immunocapture of big, non-conducting, and negatively charged bacterial cells in the close vicinity of the electrode surface, followed by signal stabilisation. The incubation of similar concentrations of *E. coli* (10^4 and 10^6 CFU mL^{-1}) with microelectrodes modified with BSA but no Ab generated significantly lower impedance variation (Figure 3 inset). This indicated that, under the present experimental conditions, low levels of bacteria non-specific adsorption occur.

A remarkably different behaviour is observed at phage-modified microelectrodes. Figure 4 shows ΔZ recorded at 233 mHz over time for a T4-modified microelectrode in the presence of *E. coli* (10^4 CFU mL^{-1}). The curve shows an initial increase of the impedance ($6x10^4$ Ω) that proceeds for about 20-25 min, followed by a short interval of signal stabilisation and an important decrease in impedance. This behaviour was consistently observed for all the chips

studied and in all the experiments performed. The initial increase in signal is due to phage-bacteria recognition and attachment in a very similar way as it happens for immunocapture. The subsequent decrease in impedance presumably happens as a consequence of phage-induced bacterial infection and lysis, which induces cell wall disruption and release of important amounts of intracellular components. As observed by Shabani et al., this event induces increase of the medium conductivity at the vicinity of the electrode surface, which contributes to decrease charge-transfer resistance (Shabani et al., 2008). On the contrary, incubation of similar concentrations of non-target *Lactobacillus* on the phage-modified microelectrodes generated only an increase ($2x10^4$ Ω for 10^4 CFU mL^{-1} *Lactobacillus*) in impedance (Figure 4). This confirmed that very low levels of bacteria non-specific adsorption take place, and that the decrease in signal observed for *E. coli* is not due to desorption or damage of the surface protein layer.

3.4. Calibration plot for *E. coli* EIS sensing at phage-modified microelectrodes

Attempts to reuse the phage-modified microelectrodes were unsuccessful because, after bacteria phage-induced lysis, chips never recovered the initial background signals and performance. The study of these microelectrodes under the optical microscope revealed that whole bacteria and bacterial fragments remained attached to the surface. It is also worth noting that, as phage infection includes injection of the viral genome into the infected cell, a single phage cannot infect more than once. For this reason, it was decided to use new phage-modified electrodes for each bacterial concentration assayed in the following experiments.

Figure 4 inset shows the calibration plot obtained for the developed biosensor exposed to increasing concentrations of target or non-target bacteria (*E. coli* and *Lactobacillus* respectively). The log-log plot of the impedance variation (ΔZ) recorded at a fixed frequency (233 mHz) versus bacterial concentration (CFU mL^{-1}) shows a linear response for *E. coli* concentrations ranging 10^4 to 10^7 CFU mL^{-1}. Detection of the binding event at a concentration of 10^3 CFU mL^{-1} was possible only after extended incubations, but generation of dual signals was not evident within 60 minutes. ΔZ were significantly higher than signals registered for the negative control bacteria for all the concentrations studied. The calibration curve was found linear with a slope of 0.13 (Ω CFU^{-1} mL). A reproducible limit of detection (LOD) of 10^4 CFU mL^{-1} was obtained.

3.5. T4- phage biosensors in water sample matrices

The rapid and specific detection of pathogenic bacteria is very important for preventing bacterial infection/contamination and for ensuring the safety of human health. Examples where rapid intervention through the detection of pathogenic bacteria is required include, for instance, the improbable event of a bioterrorism attack, the contamination of food supplies, and the contamination of water reservoirs such as pools, beaches, city water supplies and mineral water sources. This moved us to study if phage-modified microelectrodes could be successfully applied to detection of bacteria in water samples.

With this aim, mineral water was purchased from a local provider and it was inoculated with a know concentration of *E. coli* (10^4 CFU mL^{-1}). This sample was then studied by EIS over time as previously described. We recorded the impedance spectra of an interdigitated gold microelectrode functionalised with T4-phages and BSA over time after inoculation of 10^4 CFU mL^{-1} *E. coli* (data not shown). Impedance increases slowly over time until it stabilises, but the time required for signal stabilisation is significantly longer than in the experiments performed in PBS (60-70 min compared to 20-25 min). This is consistent with the fact that phages are able to bind bacteria in such a poor media, but less efficiently than when in the presence of higher concentrations of salts. This is clearly shown in Figure 5, where the variation of the absolute impedance $|Z - Z_0|$ recorded at a fixed frequency of 233 mHz is plot versus the incubation time. Under these experimental conditions, dual signals of opposite trend are not generated and decrease in impedance is not observed following signal stabilisation. This is presumably related to the fact that bacterial metabolism and growth, which already slow down at room temperature, are additionally delayed in a nutrient-deprived medium such as water. Because phages are parasites, infection cannot proceed unless bacterial metabolism works.

Figure 6 shows the variation of the absolute impedance $|Z-Z_0|$ of an interdigitated microelectrode functionalised with Ab and BSA, recorded in mineral water at a fixed frequency of 233 mHz. Compared to the previous experiment performed using phage-modified microelectrodes, the sensitivity is more pronounced with T4-phages than with antibody. Moreover, the impedance of the interdigitated microelectrodes functionalised with Ab and BSA was not stable in water. As before the increase in impedance caused by bacteria

binding is very slow in comparison with the experiment performed in PBS. Signal instability was attributed to the fact that antibodies, like most of proteins, require some salt concentration to keep their structure stable. In addition, the presence of ions is necessary for the efficient establishment of the electrostatic interactions and hydrogen bonds between Ab and their molecular targets (bacteria in this case).

According to these results, the developed T4-phage sensors are more stable than Ab sensors and could be used to detect bacteria directly in water samples, but the assay would be slower and would not provide dual signal confirmation under such conditions. Otherwise, water samples could be supplemented with salts and/or nutrients previous to their study in order to guarantee sensor performance.

4. Conclusions

In the present work, we compared the kinetic behaviour of antibody and T4-phage as bioreceptors for bacteria biosensing following their immobilisation onto gold microelectrodes by fast and random physisorption. The produced surfaces have been characterised by EIS and Fourier Transform Infra-Red Spectroscopy, and have been applied to bacteria detection by Impedance Spectroscopy. Compared to Ab, phages produced two consecutive signal trends of opposite sign that made possible in-chip signal confirmation. Furthermore, bacteria detection was also possible in water, although in this case the response was slower and did not generate dual signals.

Acknowledgments

This research is sponsored by NATO's Public Diplomacy Division in the Framework of "Science for Peace", project SFP 983115. FJDC thanks the Spanish Ministry of Science and Innovation for a Ramón y Cajal fellowship. The authors thank Biophage Pharma (Canada) and Dr. Mohamed Zourob (Canada) for providing *E. coli* and T4 phages. Additionally, this material was based on work which supported ALS by the National Science Foundation, while working at the Foundation. Any opinion, finding, and conclusions or recommendations expressed in this material are those of the authors and do not necessarily reflect the views of the National Science Foundation.

Figure Captions

Figure 1. (a) Structure and components of the T4-phage biosensor. (b) Amplified photography of a section of the interdigitated gold microelectrodes.

Figure 2. EIS spectra recorded before and after physisorption of T4-phage and BSA on interdigitated gold microelectrodes. Inset shows stability over time of physisorbed T4-phage (with BSA) on interdigitated gold microelectrodes.

Figure 3. EIS spectra recorded before and after physisorption of anti-*E. coli* polyclonal antibody on interdigitated microelectrodes. Inset shows ΔZ registered at 233 mHz over time in the presence of *E. coli* for microelectrodes modified with anti-*E. coli* Ab and BSA (caused by specific immunocapture) or only BSA (due to bacteria non-specific adsorption).

Figure 4. ΔZ registered at 233 mHz over time for phage-modified microelectrodes in the presence of 10^4 CFU mL^{-1} *E. coli* (caused by specific capture) or *Lactobacillus* (due to bacteria non-specific adsorption). (Inset) Calibration plot for detection of *E. coli* and *lactobacillus* using T4-phage interdigitated gold microelectrodes (Frequency 233 mHz).

Figure 5. Nyquist plots obtained over time for an interdigitated gold microelectrode functionalized with T4-phages and blocked with BSA in sterile mineral water after inoculation with 10^4 CFU ml^{-1} *E. coli*.

Figure.6 : Impedance variation registered at a fixed frequency of 233 mHz for the T4-phage and Ab interdigitated gold microelectrodes after inoculation of mineral water spiked with 10^4 CFU mL^{-1} *E. coli*.

References

Balasubramanian, S., Sorokulova, I.B., Vodyanoy, V.J., Simonian, A.L., 2007. Biosens. Bioelectron. 22(6), 948-955.

Baldrich, E., Laczka, O., del Campo, F.J., Munoz, F.X., 2008. Anal. Bioanal. Chem. 390(6), 1557-1562.

Bhaskaran, A., Ragavan, C.M., Sankar, R., Mohankumar, R., Jayavel, R., 2007. Cryst. Res. Technol. 42(5), 477 - 482.

Butler, J.E., 2000. Methods 22(1), 4-23.

Daniels, J.S., Pourmand, N., 2007. Electroanalysis 19(12), 1239-1257.

Das, R.D., RoyChaudhuri, C., Maji, S., Das, S., Saha, H., 2009. Biosens. Bioelectron 24(11), 3215-3222.

Heitz, F., Van Mau, N., 2002. Biochim. Biophys. Acta 1597(1), 1-11.

Kim, G., Mun, J.H., Om, A.S., 2007. J. Phys. Conf. Ser. 61(1), 555-559.

Kohli, P., Harris, J.J., Blanchard, G.J., 1998. J. Am. Chem. Soc. 120, 11962-11968.

Laczka, O., Baldrich, E., del Campo, F.J., Munoz, F.X., 2008. Anal. Bioanal. Chem 391(8), 2825-2835.

Laczka, O., Baldrich, E., Munoz, F.X., del Campo, F.J., 2008. Anal. Chem. 80(19), 7239-7247.

Lakshmanan, R.S., Guntupalli, R., Hu, J., Kim, D.-J., Petrenko, V.A., Barbaree, J.M., Chin, B.A., 2007. J. of Microbio. Methods 71(1), 55-60.

Mac Kenzie, W.R., Hoxie, N.J., Proctor, M.E., Gradus, M.S., Blair, K.A., Peterson, D.E., Kazmierczak, J.J., Addiss, D.G., Fox, K.R., Rose, J.B., et al., 1994. N. Engl. J.of Med. 331(3), 161-167.

Muñoz-Berbel, X., Godino, N., Laczka, O., Baldrich, E., Muñoz, F.X., del Campo, F.J., 2008. Principles of Bacterial Detection: Biosensors, Recognition Receptors and Microsystems. Zourob, M., Elwary, S., Turner, A., Springer. 15**:** 339-374.

Norrung, B., Buncic, S., 2008. Meat Sci.78(1-2), 14-24.

Panke, O., Balkenhohl, T., Kafka, J., Schafer, D., Lisdat, F., 2008. Adv. Biochem. Eng. Biotechnol. 109, 195-237.

Pournaras, A.V., Koraki, T., Prodromidis, M.I., 2008. Anal. Chim. Acta 624(2), 301-307.

Radke, S.A., Alocilja, E.C., 2005. Biosens. Bioelectron 20(8), 1662-1667.

Radke, S.M., Alocilja, E.C., 2005. IEEE Sens. J. 5(4), 744-750.

Ruan, C., Yang, L., Li, Y., 2002. Anal. Chem. 74 (18), 4814-4820.

Shabani, A., Zourob, M., Allain, B., Marquette, C.A., Lawrence, M.F., Mandeville, R., 2008. Anal. Chem. 80(24), 9475-9482.

Tauxe, R.V., 2002. Int. J. Food Microbiol. 78(1-2), 31-41.

U.S. Centers for Disease Control and Prevention. Atlanta, 2006. World Water Forum 4 Update.

Varshney, M., Li, Y., Srinivasan, B., Tung, S., 2007. Sens. Actuators, B: Chem. 128(1), 99-107.

Varshney, M., Li, Y.B., 2009. Biosens. Bioelectron 24(10), 2951-2960.

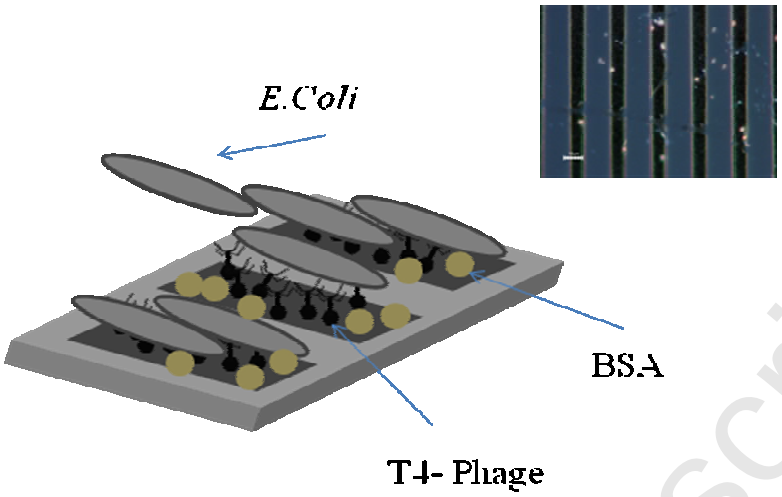

Figure 1

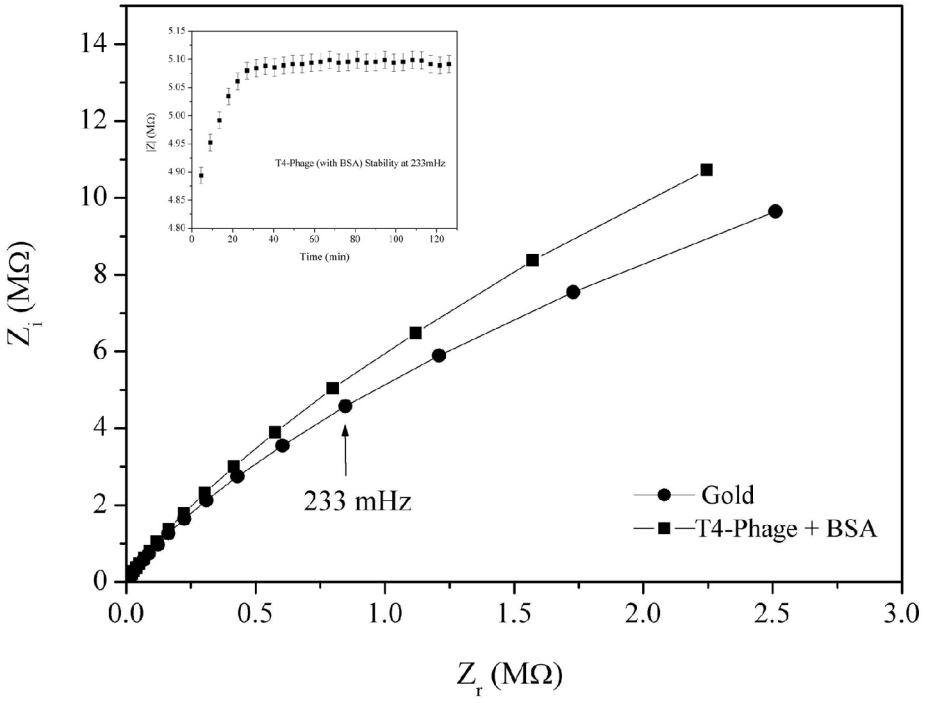

Figure 2

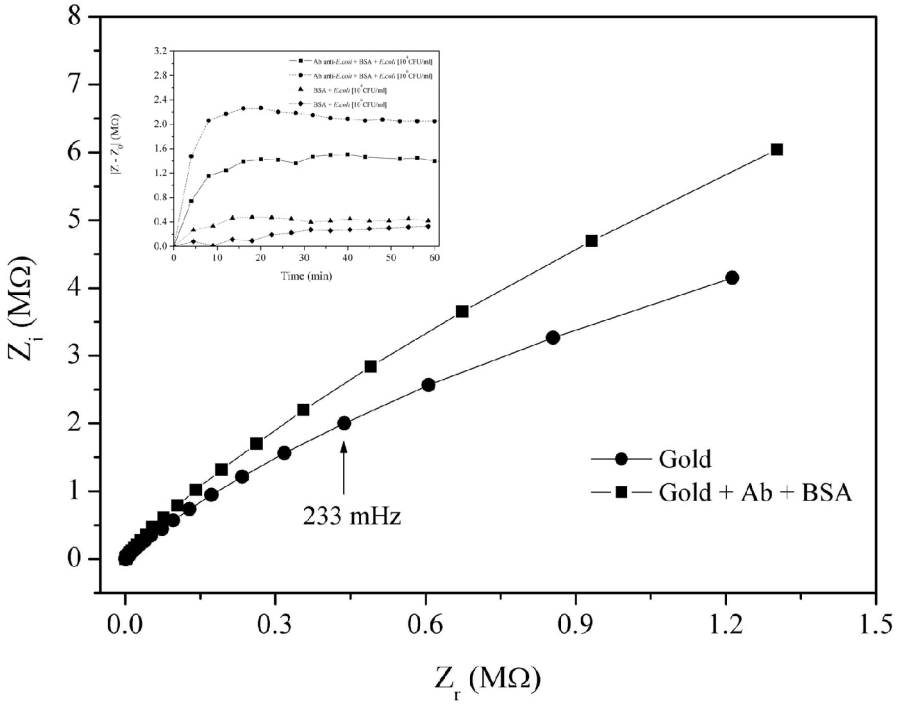

Figure 3

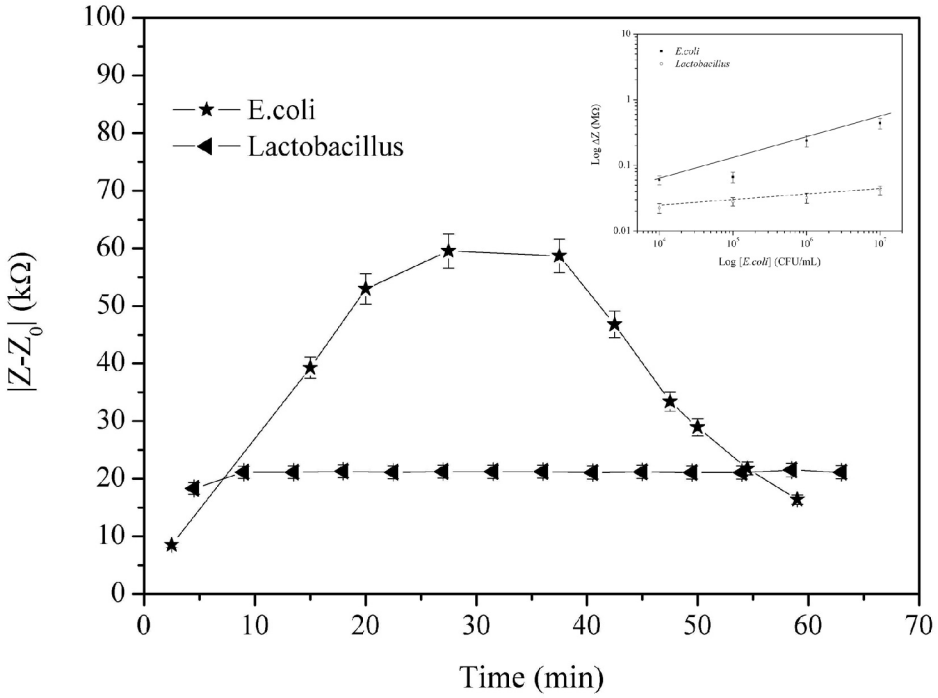

Figure 4

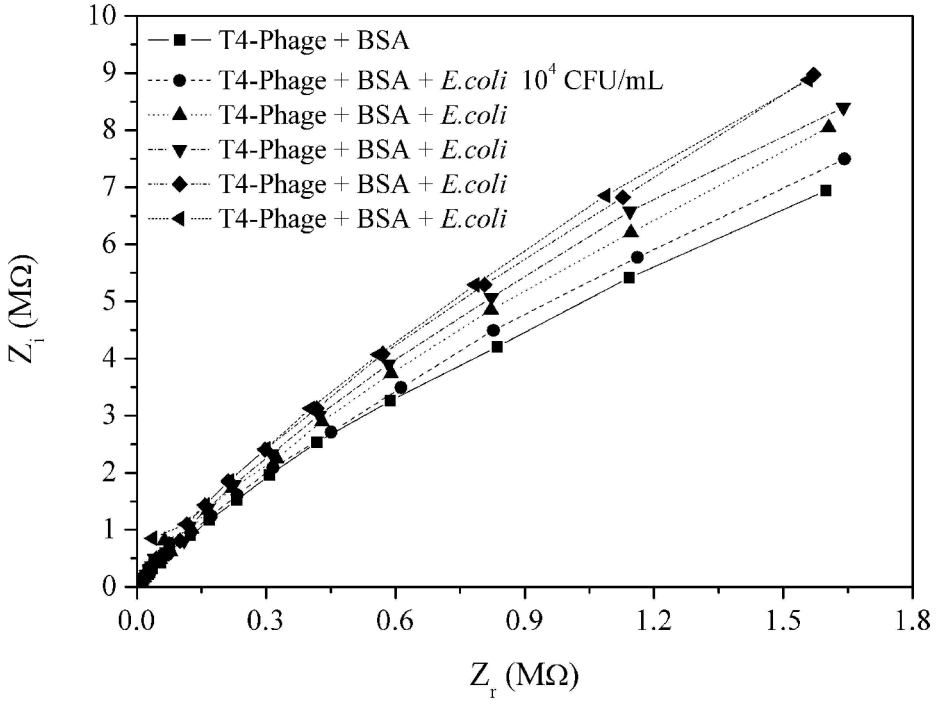

Figure.5

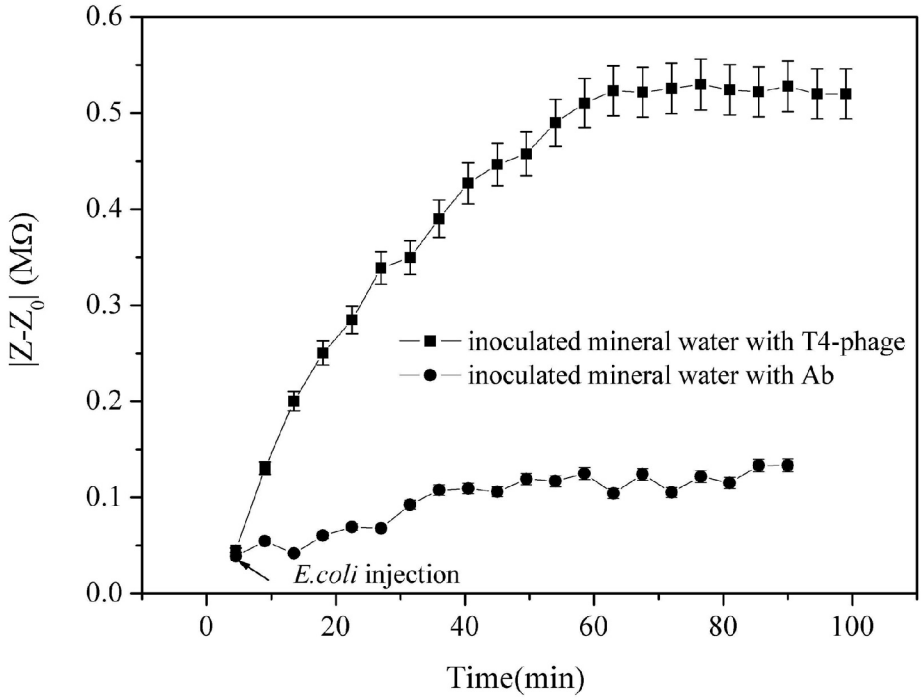

Figure 6